Pyrene acetylide nucleotides in GNA: probing duplex formation and sensing of copper(II) ions†

Hui Zhou,[a] Xiaoyan Ma,[b,c] Jianpian Wang[b] and Lilu Zhang*[a]

Received 6th January 2009, Accepted 5th March 2009
First published as an Advance Article on the web 14th April 2009
DOI: 10.1039/b900167k

The synthesis and evaluation of GNA duplexes containing fluorescent pyrene and pyrene acetylide nucleotides is reported. Interestingly, only the pyrene acetylides, but not the related plain pyrene nucleotides, form strong excimers upon stacking in glycol nucleic acid (GNA) duplexes. The ability of the large pyrene acetylide nucleotide to be accommodated in GNA duplexes opposite an abasic site was investigated by molecular modeling. The interstrand pyrene acetylide excimer formation was used to monitor GNA duplex formation and was applied to the design of a copper(II)-selective "turn-on" fluorescence sensor.

Introduction

DNA duplexes constitute a very popular scaffold for assembling functional architectures in a predictable fashion based on Watson–Crick base pairing. However, DNA itself lacks interesting functionality and therefore different strategies for generating modified nucleic acids have been developed over the last decades. Usually, phosphoramidites of modified nucleotides are incorporated into DNA by automated solid phase synthesis. This often requires the tedious synthesis of phosphoramidites of 2′-deoxynucleosides. In order to address the problem of time consuming synthesis of nucleotide building blocks, the Meggers group recently developed a glycol nucleic acid (GNA) which combines the ability of highly stable duplex formation with a structurally simplified propylene glycol backbone (Fig. 1).[1] A recently published crystal structure confirms that duplex formation follows the established Watson–Crick base pairing.[2] GNA may be advantageous for the design of functional architectures since modified GNA nucleotide building blocks are accessible in an economical fashion starting from commercially available glycidol. Having this simplified backbone in hand, an interesting next goal will be to use GNA as simplified general duplex scaffold for the design of self-assembled and self-organized architectures. Towards this long term goal, the first step must be the development of strategies for the synthesis of modified GNA nucleotides and their evaluation in the context of GNA duplexes.

Pyrenes have been used extensively in DNA because of their high quantum yields, efficient planar aromatic stacking and their ability to form excimer emission upon stacking.[3,4] Here we report for the first time the synthesis and evaluation of GNA duplexes containing fluorescent pyrene nucleotides. We show that pyrene acetylides, but not the related pyrene nucleotides itself, form strong excimers in GNA duplexes and can be used to readout GNA duplex formation. As an application of this excimer emission, we have developed a sensitive GNA-based fluorescent sensor for copper(II) ions.

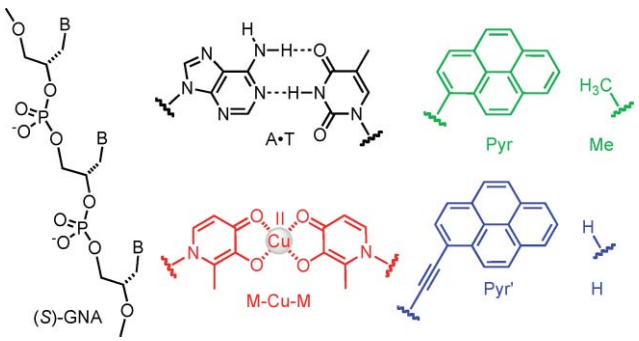

Fig. 1 Constitution of (*S*)-GNA and the base pairs used in this study.

Results and discussion

Synthesis of pyrene and pyrene acetylide GNA nucleotides

As fluorescent GNA nucleotide building blocks we chose **Pyr** and **Pyr′** in which the natural nucleobases of propylene glycol nucleotides are replaced by pyrene and pyrene-1-acetylide moieties as shown in Fig. 1. The synthesis of these two building blocks is shown in Scheme 1. 1-Bromopyrene (**1**) was converted into 1-pyrenyllithium by reaction with *n*-BuLi at −78 °C in THF. The lithium species was subsequently transmetallated into a Grignard reagent by treatment with freshly prepared $MgBr_2$ (synthesized from Mg turnings and 1, 2-dibromoethane). In the presence of CuI, the resulting solution underwent a regioselective and stereospecific ring-opening with dimethoxytrityliated (*S*)-glycidol **2** to afford the alcohol **3** in 50% yield. The subsequent reaction with the phosphoramidite reagents **4** afforded **5** in 84%. This protocol

[a]*Fachbereich Chemie, Philipps-Universität Marburg, Hans-Meerwein-Straße, D-35032, Marburg, Germany. E-mail: zhangl@staff.uni-marburg.de; Fax: +49-6421-2822189; Tel: +49-6421-2825600*
[b]*Beijing National Laboratory for Molecular Science, State Key Laboratory of Molecular Reaction Dynamics, Institute of Chemistry, Chinese Academy of Science, No.2, First North Street, Zhongguancun, 100190, Beijing, China*
[c]*Graduate School of Chinese Academy of Sciences, 100049, Beijing, China*
† Electronic supplementary information (ESI) available: Fluorescence properties of pyrene and pyrene acetylide nucleotides in GNA at different concentrations, metal ion-selectivity at different temperatures, Maldi-TOF data of all oligonucleotides, NMR spectra of compounds **3**, **5**, **7** and **8**. See DOI: 10.1039/b900167k

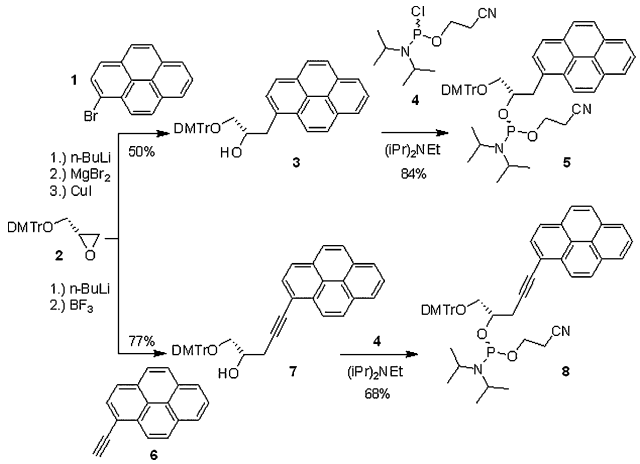

Scheme 1 Synthesis of pyrene phosphoramidites **5** and **8**.

involving a metallation/transmetallation sequence is general and has been applied to the synthesis of other aromatic C-nucleosides (data not shown).

As for the synthesis of the pyrene acetylide GNA nucleotide, pyrene-1-acetylene **6** was first deprotonated with *n*-BuLi and then reacted with glycidol **2** in the presence of BF_3 to afford compound **7** in 77% yield, followed by the reaction with **4** in the presence of Hünig's base to afford the pyrene acetylide phosphoramidite **8** in 68% yield.

Altogether, the pyrene phosphoramidite building blocks **5** and **8** were synthesized in just two steps from dimethoxytritylated (*S*)-glycidol with overall yields of 42% and 52%, respectively, demonstrating the usefulness of the GNA backbone for the economical synthesis of modified nucleotides.

Pyrene-containing GNA duplexes

Pyrene nucleotides have been demonstrated to fit into the base stacking of nucleic acid duplexes by arranging them opposite abasic sites in order to accommodate for their expanded size.[3a] We therefore chose GNA abasic sites based on ethylene glycol (**H**) and (*S*)-(+)-1,2-propanediol (**Me**) shown in Fig. 1. GNA oligonucleotides containing the pyrene nucleotides **Pyr** and **Pyr′**, as well as the abasic sites **H** and **Me** (Fig. 1), were synthesized on CPG supports with standard protocols for 2-cyanoethyl phosphoramidites and purification was performed by HPLC.

We started with incorporating the pyrene nucleotide **Pyr** into 16mer GNA oligonucleotides. Table 1 reveals that **Pyr** was slightly better accommodated opposite a methylated abasic site **Me** (Table 1, duplex D3) compared to the abasic site **H** (Table 1, duplex D2), being only by 4 °C less stable than an A:T base pair at the same position (Table 1, duplex D1). Encouraged by these stabilities, we synthesized duplexes D4-D7 (Table 1), having incorporated all permutations of adjacent **Pyr-Me** base pairs in order to investigate excimer fluorescence formation in GNA duplexes. Table 1 demonstrates that all systems form stable duplexes at room temperature. However, excimer emission results turned out to be disappointing for pyrene-containing duplexes. Upon excitation at 315 nm, the duplexes D4-D6, containing each two adjacent pyrene nucleobases, give overall low fluorescence quantum yields with low emissions at 395 nm (regular emission) as well as low emissions at

Table 1 Properties of GNA duplexes containing pyrene and pyrene acetylide nucleotides[a]

3′-TAAAAATNNTAATATT-2′
2′-ATTTTTANNATTATAA-3′

Name	Duplexes	T_m (°C)	ΔT_m (°C)	Excimer[b]
D1	A A T T	54	—	—
D2	**H** A **Pyr** T	49	–5	none
D3	**Me** A **Pyr** T	50	–4	none
D4	**Me Me** **Pyr Pyr**	33	–21	weak
D5	**Pyr Pyr** **Me Me**	42	–12	weak
D6	**Me Pyr** **Pyr Me**	36	–18	weak
D7	**Pyr Me** **Me Pyr**	43	–11	none
D8	**Pyr′** A **Me** T	50	–4	none
D9	**Pyr′** A **H** T	51	–3	none
D10	**H H** **Pyr′ Pyr′**	32	–22	strong
D11	**Pyr′ Pyr′** **H H**	39	–15	strong
D12	**H Pyr′** **Pyr′ H**	34	–20	medium
D13	**Pyr′ H** **H Pyr′**	41	–13	strong

[a] Conditions: 10 mM sodium phosphate, 100 mM NaCl, 2 μM duplex. [b] Excitation at 315 nm with cutoff filter at 325 nm. Fluorescence at 460 nm taken as indicator for excimer fluorescence.

460 nm (excimer emission) as shown in Fig. 2A, compared to the duplex D3 harboring a single pyrene (strong regular emission at 395 nm) and a **Pyr-Pyr**-containing single strand (strong excimer emission at 460 nm). Moreover, duplex D7 does not yield any excimer emission at all. This latter result can be explained with the strong nucleobase-backbone inclination in GNA duplexes which should result in only a very weak stacking of the two pyrene

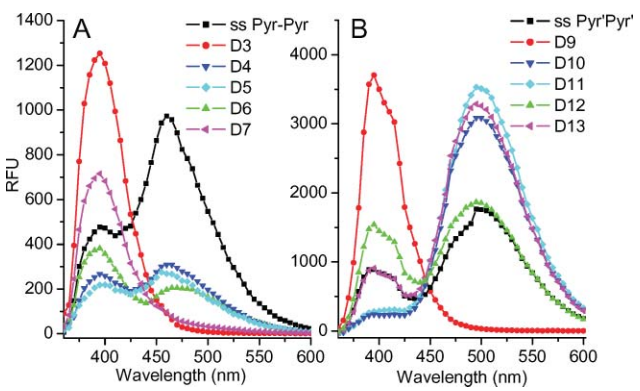

Fig. 2 Fluorescene properties of A) pyrene and B) pyrene acetylide nucleotides in GNA. Conditions: 10 mM sodium phosphate, 100 mM NaCl, pH 7.0, and 8 μM of each strand of a duplex (D3-D7 and D9-D13) or 8 μM for the single strands 3′-TAAAAAT**PyrPyr**TAATATT-2′ and 3′-TAAAAAT**Pyr′Pyr′**TAATATT-2′.

nucleobase in duplex D7. However, the weak excimer emission of duplexes D4-D6, in combination with the overall low fluorescence quantum yields, remains unclear.

Pyrene acetylide-containing GNA duplexes

We next investigated the pyrene acetylide nucleotide **Pyr′** in the context of GNA duplexes. Interestingly, although significantly larger than **Pyr**, **Pyr′** fits well into GNA duplexes opposite the abasic sites **H** (T_m = 51 °C, Table 1, duplex D9) and **Me** (T_m = 50 °C, Table 1, duplex D8), with the base pair **Pyr′-H** being only by 3 °C less stable than an A:T base pair at the same position (Table 1, duplex D1). Subsequently, duplexes with all permutations of two adjacent **Pyr′-H** base pairs were synthesized (Table 1, duplexes D10-D13), all resulting in thermally stable duplexes at room temperature.

Fortunately, using the pyrene acetylide **Pyr′** instead of the pyrene nucleotide **Pyr**, the fluorescence properties were dramatically improved. Fig. 2B demonstrates that in particular the duplexes D10, D11, and D13 yield very strong excimer emission intensities upon excitation at 315 nm which exceed the excimer emissions of the corresponding pyrene duplexes D4, D5, and D7 (Fig. 2A) by around 10-fold. Most interestingly, whereas D10 and D11 contain adjacent pyrene acetylides in the same strand, duplex D13 provides strong excimer fluorescence despite the pyrene acetylide nucleotides **Pyr′** being in opposite strands. The arrangement of **Pyr′** nucleotides in opposite strands in D13 therefore allows to monitor duplex formation by following the intensity of excimer emission relative to the regular emission of the single strands. It is noteworthy that concentration-dependent control experiments confirmed that at the duplex concentrations of 8 μM used in these experiments, no intermolecular exciplexes were observed.

Overall, compared to pyrene-containing duplexes (**Pyr**), pyrene acetylide-containing duplexes (**Pyr′**) form much stronger excimers. Most likely, the superior behaviour of **Pyr′** in GNA duplexes is due to a combination out of structural effects, influencing the stacking of adjacent **Pyr′** nucleobases, and electronic effects due to the conjugation of the aromatic pyrene with the acetylide π-system.

Molecular modeling

Molecular modeling was carried out in order to understand the accommodation and fluorescence properties of pyrene acetylides in GNA. An 8mer containing duplex with an arrangement of **Pyr′-H** base pairs in analogy to duplex D13 (Table 1) was first constructed. A full geometry optimization was performed in *vacuum* using HyperChem (Version 7.5, Hypercube, Inc.) with the AMBER[6] force field. The optimization took 1913 steps to reach a satisfactory convergence. The steepest descent algorithm and the terminating gradient 0.1 kcal mol^{-1} Å^{-1} were employed during the optimization. A well ordered duplex structure was obtained (Fig. 3). The two pyrene acetylide nucleobases are found to be in an almost perfect stacking configuration with an inter-plane distance of 3.3 Å, suggesting a perfect match of the pyrene acetylide base within the frame of GNA. Apparently, the conjugated pyrene ring as well as the acetylide triple bond all play a role in resulting in the observed strong excimer formation.

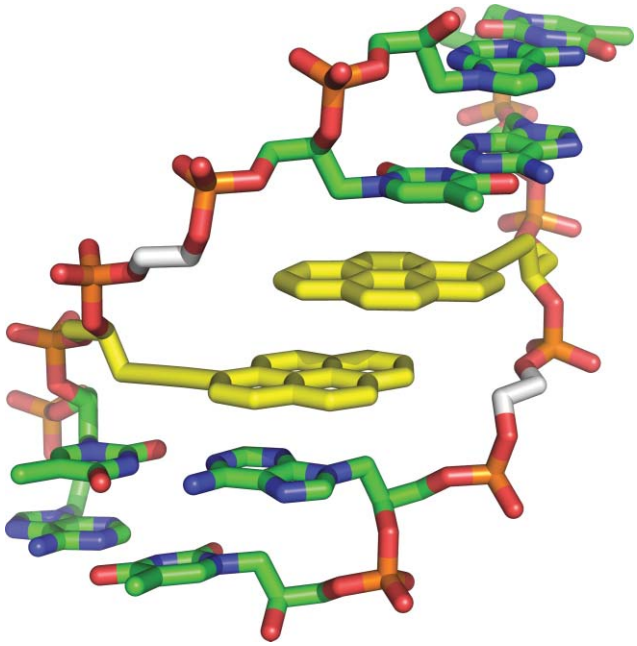

Fig. 3 AMBER force field model of an 8mer duplex containing adjacent pyrene acetylides in opposite strands. The pyrene acetylide nucleotides are shown in yellow and the abasic sites in white.

Design of a GNA-based copper ion sensor

As an application of excimer emission upon duplex formation with pyrene acetylide containing GNA strands, we envisioned to develop a metal ion sensor by additionally incorporating a metal-mediated base pair. Fig. 4 shows the designed duplex D14 which includes two **Pyr′-H** base pairs arranged in analogy to duplex D13 (Table 1) in addition to a metal-mediated hydroxypyridone homo-base pair **M-M** (see Fig. 1 for the molecular structure). The hydroxypyridone homo-base pair is known to

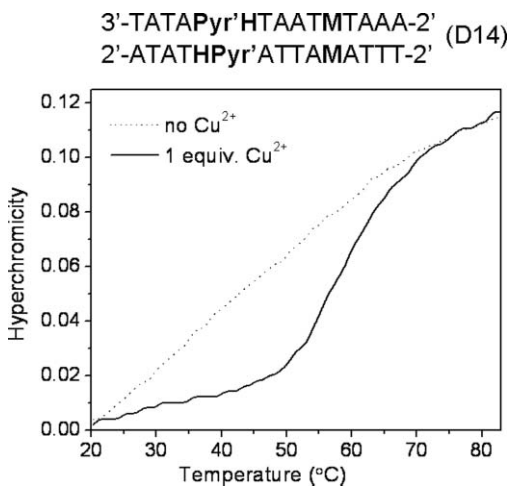

Fig. 4 Copper(II)-dependent UV-melting curves of duplex D14. Conditions: 10 mM sodium phosphate, 50 mM NaCl, pH 7.0, and 2 μM each strand of a duplex D14, in which **M** is a hydroxypyridone nucleobase (see Fig. 1).

increase DNA and GNA duplex stability in the presence of Cu^{2+} ions.[5,7] This effect has recently been demonstrated to be even significant stronger in GNA duplexes compared to DNA with an increase in duplex stability in the presence of Cu^{2+} by around 30 °C.[7]

Thus, as expected, in the absence of Cu^{2+} ions, duplex D14 is strongly destabilized not showing any cooperative melting behaviour upon analysis with temperature-dependent UV-melting at 260 nm (Fig. 4). However, after the addition of only one equivalent of $CuCl_2$, D14 exhibits a sigmoidal melting curve with a melting point (T_m) of 55 °C (10 mM sodium phosphate, 50 mM NaCl).

Next, we analyzed the fluorescence properties of the duplex D14 in the presence and absence of $CuCl_2$. In the absence of Cu^{2+} (40 °C, 10 mM sodium phosphate, 50 mM NaCl, 2 μM each strand), almost exclusively the regular emission at around 400 nm is observed, indicating that the two strands of D14 are mainly dissociated under these conditions (Fig. 5A, blue line). In contrast, upon the addition of just one equivalent of Cu^{2+}, the regular pyrene acetylide emission at 400 nm decreases whereas the excimer emission increases strongly (Fig. 5A and 5B, red line). Using the ratio of regular emission (400 nm) and excimer emission (500 nm) as a measure for the copper effect, this ratio changes by a factor of 14-fold in presence of one equivalent of Cu^{2+}. A titration of Cu^{2+} to a denatured duplex D14 reveals that excimer emission increases with increasing amount of Cu^{2+} until around one equivalent of Cu^{2+} is reached, with only a marginal further increase upon addition of more Cu^{2+}. This is in agreement with the notion that one equivalent is needed in order to stabilize the duplex D14 through a copper(II)-mediated hydroxypyridone base pair.

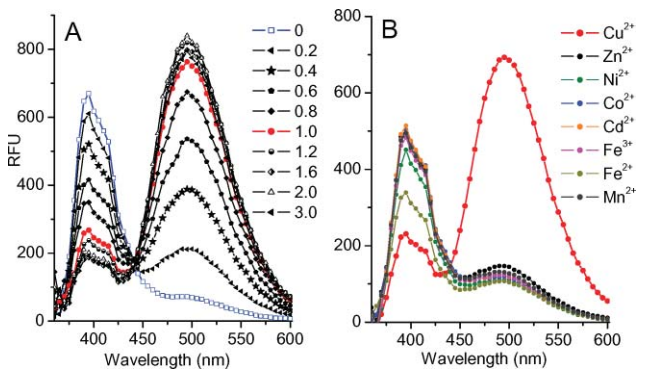

Fig. 5 Copper(II)-sensing with GNA. A) Titration. Conditions: 10 mM sodium phosphate, 50 mM NaCl, pH 7.0, 2 μM each strand of a duplex D14, 40 °C. B) Metal ion-selectivity. Conditions: 10 mM sodium phosphate, 50 mM NaCl, pH 7.0, and 2 μM each strand of duplex D14, 50 °C.

In contrast, other metal ions such as Ni^{2+}, Co^{2+}, Zn^{2+}, Cd^{2+}, Mn^{2+} or $Fe^{2/3+}$ do not show any effect at the optimized temperature of 50 °C (Fig. 5B), thus demonstrating the selectivity of this sensor for Cu^{2+} ions (see supporting information for different temperatures). It is noteworthy that fluorescent copper ion sensors typically "turn-off" upon Cu^{2+} binding due to the quenching properties of the paramagnetic copper(II) ions, whereas selective "turn-on" sensors such as the GNA duplex D14 are rare.[8]

Conclusions

In summary, we here demonstrated that GNA duplexes are a promising structural scaffold which, upon the introduction of modifications, allow to program desired properties. Pyrene acetylide GNA nucleotides enable to monitor duplex formation by excimer fluorescence detection and this was applied to the design of a fluorescent copper(II) ion sensor.

Experimental

Synthesis of pyrene GNA phosphoramidites

NMR spectra were recorded on a Brucker AVANCE 300 and Brucker DRX 500. Low-resolution mass spectra were obtained on an LC platform from Agilent using ESI technique. High-resolution mass spectra were obtained on a Thermo Finnigan LTQ FT instrument using APCI ionization. Infrared spectra were recorded on a Brucker "Alpha-P" FT-IR spectrometer. HPLC was performed using an Agilent technologies 1200 series instrument with fraction collection. All non-aqueous operations were carried out under dry nitrogen atmosphere. Solvents and reagents were used as supplied from Aldrich, Alfa Aesar or Acros. Abasic site nucleotides were synthesized as reported.[9,10]

Compound 3. To a solution of 1-bromopyrene (2.56 g, 9.14 mmol) in THF (20 mL) at −78 °C was added dropwise *n*-BuLi in hexane (7.2 mL, 11.5 mmol) over 20 min. After stirring for 30 min, a suspension of freshly prepared $MgBr_2$ [made as follows: to a suspension of magnesium turnings (0.44 g, 18.3 mmol) in THF (37 mL) was added dropwise 1,2-dibromoethane (1.62 mL, 18.7 mmol)] was added dropwise over 20 min. The resulting solution was first kept at −78 °C with stirring for 30 min and then warmed to 0 °C and stirring was continued for another 30 min. The solution was then cooled to −40 °C and stirred for 1 hour. To the resulting solution was added a slurry of CuI (0.23 g, 1.22 mmol) in THF (2.44 mL). Then, the epoxide **2** (2.37 g, 6.1 mmol) in THF (12 mL) was added and stirring was continued at the same temperature for 2 hours. The solution was warmed to room temperature, stirred for another 1 hour, and the reaction mixture was poured into saturated $NaHCO_3$ and extracted with CH_2Cl_2 (3 × 50 mL). The combined organic extracts were dried over anhydrous Na_2SO_4, concentrated *in vacuo*, and the resulting oil was purified by chromatography over silica gel, first eluting with hexanes/ethyl acetate/triethylamine (5:1:0.01), then with hexanes/ethyl acetate/triethylamine (3:1:0.01), affording compound **3** as a light yellow foam (1.79 g, 50%). ^{1}H-NMR (300 MHz, $CDCl_3$): δ = 8.26 (d, J = 9.3 Hz, 1H), 8.18 (d, J = 7.8 Hz, 2H), 7.98–8.09 (m, 5H), 7.79 (d, J = 7.8 Hz, 1H), 7.48 (m, 2H), 7.27–7.35 (m, 6H), 7.22 (m, 1H), 6.79 (dd, J = 2.3, 9.0 Hz, 4H), 4.20 (m, 1H), 3.74 (d, J = 2.0 Hz, 6H), 3.58 (dd, J = 6.0, 13.9 Hz, 1H), 3.47 (dd, J = 7.3, 13.7 Hz, 1H), 3.28 (m, 2H), 2.37 (d, J = 4.3 Hz, 1H). ^{13}C NMR (75 MHz, $CDCl_3$): δ = 158.65, 145.02, 136.13, 132.46, 131.51, 130.99, 130.31, 130.22, 130.20, 129.35, 128.41, 128.30, 127.97, 127.60, 127.51, 126.96, 125.97, 125.18, 125.09, 125.04, 124.94, 124.81, 123.58, 113.26, 86.52, 72.31, 67.00,

55.29, 37.86. IR (thin film): ν = 3037, 2929, 2834, 1605, 1583, 1507, 1461, 1444, 1299, 1175, 1154, 1069, 1031, 980, 907, 840, 827, 791, 754, 726, 703, 682, 647 and 582 cm^{-1}. HRMS: *m/z* [M^+] calcd for $C_{40}H_{34}O_4$: 578.2452; found: 578.2449.

Compound 5. To a solution of **3** (1.79 g, 3.09 mmol) and *N*,*N*-diisopropylethylamine (3.09 mL, 16.4 mmol) in CH_2Cl_2 (52 mL) was added compound **4** (1.37mL, 6.18 mmol). After 2 h, the reaction mixture was poured into sat. aq. $NaHCO_3$ (40 mL) and extracted with CH_2Cl_2 (3 × 40 mL). The combined organic extracts were dried over anhydrous Na_2SO_4, concentrated *in vacuo*, and the resulting oil was purified by chromatography over silica gel eluting with hexanes/ethyl acetate/triethylamine (5:1:0.01), affording compound **5** as a light yellow foam (2.02 g, 84%). ^{31}P NMR (121.5 MHz, $CDCl_3$): δ = 147.53, 147.16. HRMS: *m/z* [M + H^+] calcd for $C_{49}H_{52}N_2O_5P_1$: 779.3608; found: 779.3602.

Compound 7. To a solution of **6**[11] (300 mg, 1.33 mmol) in THF (8 mL) at −78 °C was added slowly *n*-BuLi in hexane (0.84 mL, 1.34 mmol). After stirring for 10 min at −78 °C, $BF_3{\cdot}Et_2O$ (0.17 mL, 1.33 mmol) was added dropwise and the stirring continued for another 5 min. The solution of compound **2** (498.6 mg, 1.33 mmol) in THF (5 mL) was then added slowly at −78 °C. Stirring was continued for another 15 min at −78 °C, then the reaction was quenched with saturated $NaHCO_3$ (50 mL) at −78 °C. The mixture was extracted with CH_2Cl_2 (3 × 40 mL). The combined organic layers were dried over anhydrous Na_2SO_4, concentrated *in vacuo*, and the resulting red oil was purified by chromatography over silica gel eluting with hexanes/ethyl acetate/triethylamine (3:1:0.01), affording compound **7** as a light yellow foam (0.55 g, 68%). ^1H NMR (300 MHz, $CDCl_3$): δ = 8.44 (d, *J* = 9.1 Hz, 1H), 8.20 (m, 2H), 7.96–8.10 (m, 6H), 7.52 (m, 2H), 7.40 (m, 4H), 7.31 (m, 2H), 7.21 (m, 1H), 6.81 (d, *J* = 8.9 Hz, 4H), 4.19 (m, 1H), 3.67 (s, 6H), 3.48 (m, 2H), 2.98 (d, *J* = 6.3 Hz, 2H), 2.60 (d, *J* = 5.3 Hz, 1H). ^{13}C NMR (75 MHz, $CDCl_3$): δ = 158.46, 144.85, 135.84, 135.83, 131.78, 131.11, 130.95, 130.77, 130.05, 129.66, 128.08, 127.84, 127.78, 127.09, 126.79, 126.05, 125.42, 125.33, 125.29, 124.29, 124.26, 124.18, 118.05, 113.14, 91.53, 86.29, 81.76, 69.74, 66.15, 54.98, 25.34. IR (thin film): 3037, 2929, 2834, 1605, 1581, 1507, 1461, 1442, 1299, 1246, 1174, 1072, 1031, 905, 845, 826, 790, 754, 717, 701, 681, 613, 582 and 543 cm^{-1}. HRMS: *m/z* [M^+] calcd for $C_{42}H_{34}O_4$: 602.2452; found: 602.2429.

Compound 8. To a solution of **7** (1.0 g, 1.66 mmol) and *N*,*N*-diisopropylethylamine (1.66 mL, 8.83 mmol) in CH_2Cl_2 (27 mL) was added compound **4** (0.55 mL, 2.49 mmol). After 2 h, the reaction mixture was poured into sat. aq. $NaHCO_3$ (30 mL) and extracted with CH_2Cl_2 (3 × 30 mL). The combined organic layers were evaporated and the residue was purified by chromatography over silica gel eluting with hexanes/ethyl acetate/triethylamine (3:1:0.01), affording **7** as a light yellow foam (1.03 g, 77%). ^{31}P NMR (161.9 MHz, $CDCl_3$): δ = 147.85, 147.80. HRMS: *m/z* [M + H^+] calcd for $C_{51}H_{51}N_2O_5P_1$: 803.3608; found: 803.3570.

Nucleic acid chemistry

Oligonucleotide synthesis and purification. All oligonucleotides were prepared on an ABI 394 DNA/RNA Synthesizer on a 1 micromole scale. A standard protocol for 2-cyanoethyl phosphoramidites (0.1 M) was used, except that the coupling was extended to 3 minutes. After the trityl-on synthesis, the resin was incubated with conc. Aq. NH_3 at 55 °C for 12 h and then evaporated. The tritylated oligonucleotides were purified by C18 reverse phase HPLC (Merck LiChroCART 250 × 4.6 mm, Purospher STAR RP-18e) with 0.05 M aq. TEAA and MeCN as the eluent (gradient: 15–80% MeCN in 20 min). The oligonucleotides were then detritylated with 80% AcOH for 20 min, precipitated with *i*-PrOH after addition of NaOAc, and again purified by HPLC. In an alternative protocol, the tritylated oligonucleotides were purified by Water Sep-Pak classic C18 cartridges. The trityl-off oligonucleotides were purified by using a Waters Xterra column (MS C18, 4.6 × 50 mm) at 55 °C with 0.05 M aq. TEAA and MeCN as the eluent. The identities of all oligonucleotides were confirmed by MALDI–TOF MS.

Thermal denaturation. The melting studies were carried out in 1 cm path length quartz cells (total volume 325 µL; 200 µL sample solutions were covered by mineral oil) on a Beckman 800 UV-VIS spectrophotometer equipped with a thermo-programmer. Melting curves were monitored at 260 nm with a heating rate of 1 °C/min. Melting temperatures were calculated from the first derivatives of the heating curves. Experiments were performed in duplicate and mean values were taken.

Fluorescence measurements. The experiments were performed in 96-well plates on a Molecular Devices SpectraMax M5 with excitation at 315 nm and a cutoff filter at 325 nm. The experiments with pyrene and pyrene acetylide-containing duplexes were performed in 10 mM sodium phosphate, 100 mM NaCl, pH 7.0, and the concentration of each GNA strand was 8 µM. For copper sensor experiments, duplex D14 (2 µM of each strand) was dissolved in 10 mM sodium phosphate, 50 mM NaCl, ph 7.0.

Acknowledgements

We thank the Philipps-University Marburg for financial support and Prof. Dr. Eric Meggers and Mark K. Schlegel for a generous gift of the hydroxypyridone phosphoramidite and helpful discussions.

References

1 (*a*) L. Zhang, A. Peritz and E. Meggers, *J. Am. Chem. Soc*, 2005, **127**, 4171; (*b*) L. Zhang, A. E. Peritz, P. J. Carroll and E. Meggers, *Synthesis*, 2006, **4**, 645; (*c*) M. K. Schlegel, A. Peritz, K. Kittigiwittana, L. Zhang and E. Meggers, *ChemBioChem*, 2007, **8**, 927.
2 M. K. Schlegel, L.-O. Essen and E. Meggers, *J. Am. Chem. Soc*, 2008, **130**, 8158.
3 (*a*) T. J. Matray and E. T. Kool, *J. Am. Chem. Soc*, 1998, **120**, 6191; (*b*) F. D. Lewis, Y. Zhang and R. L. Letsinger, *J. Am. Chem. Soc*, 1997, **119**, 5451; (*c*) E. M-Enthart and H.-A. Wagenknecht, *Angew. Chem. Int. Ed*, 2006, **45**, 3372; (*d*) V. L. Malinovskii, F. Samain and R. Häner, *Angew. Chem. Int. Ed*, 2007, **46**, 4464; (*e*) A. Okamoto, K. Kanatani and I. Saito, *J. Am. Chem. Soc*, 2004, **126**, 4820.
4 (*a*) A. Okamoto, Y. Ochi and I. Saito, *Chem. Commun*, 2005, 1128; (*b*) J. Barbaric and H.-A. Wagenknecht, *Org. Biomol. Chem*, 2006, **4**, 2088; (*c*) I. V. Astakhova, A. D. Malakhov, I. A. Stepanova, A. S. Paramonov and V. A. Korshun, *Biocojugate Chem*, 2007, **18**, 1972.
5 K. Tanaka, A. Tengeiji, T. Kato, N. Toyama, M. Shiro and M. Shionoya, *J. Am. Chem. Soc*, 2002, **124**, 12494.

6 W. D. Cornell, P. Cieplak, C. I. Bayly, I. R. Gould, K. M. Merz, Jr., D. M. Ferguson, D. C. Spellmeyer, T. Fox, J. W. Caldwell and P. A. Kollman, *J. Am. Chem. Soc.*, 1995, **117**, 5179.
7 M. K. Schlegel, L. Zhang, N. Pagano and E. Meggers, *Org. Biomol. Chem.*, 2009, DOI: 10.1039.
8 (*a*) A. Torrado, G. K. Walkup and B. Imperiali, *J. Am. Chem. Soc*, 1998, **120**, 609; (*b*) K. Rurack, M. Kollmannsberger, U. R-Genger and J. Daub, *J. Am. Chem. Soc*, 2000, **122**, 968; (*c*) R. Krämer, *Angew. Chem. Int. Ed*, 1998, **37**, 772; (*d*) A. Mokhir, A. Kiel, D.-P. Herten and R. Krämer, *Inorg. Chem*, 2005, **44**, 5661; (*e*) L. Zeng, E. W. Miller, A. Pralle, E. Y. Isacoff and C. J. Chang, *J. Am. Chem. Soc*, 2006, **128**, 10.
9 (*a*) F. Ferreira, A. Meyer, J.-J. Vasseur and F. Morvan, *J. Org. Chem.*, 2005, **70**, 9198; (*b*) S. Mahajan, P. Kumar and K. C. Gupta, *Bioconjugate Chem*, 2006, **17**, 1184.
10 (*a*) R. Fathi, M. J. Rudolph, R. G. Gentles, R. Patel, E. W. Macmillan, M. S. Reitman, D. Pelham and A. F. Cook, *J. Org. Chem.*, 1996, **61**, 5600; (*b*) M.-L. Fontanel, H. Bazin and R. Teoule, *Nucleic Acids Research*, 1994, **22**, 2022.
11 M. Hissler, A. Harriman, A. Khatyr and R. Ziessel, *Chem Eur. J.*, 1999, **5**, 3366.

